



Aalborg Universitet

AALBORG UNIVERSITY  
DENMARK

## Amplitude versus spatially modulated electrotactile feedback for myoelectric control of two degrees of freedom

Garenfeld, Martin Alexander; Mortensen, Christian Korfitz; Štrbac, Matija; Dideriksen, Jakob L; Dosen, Strahinja

*Published in:*  
Journal of Neural Engineering

*DOI (link to publication from Publisher):*  
[10.1088/1741-2552/aba4fd](https://doi.org/10.1088/1741-2552/aba4fd)

*Creative Commons License*  
CC BY-NC-ND 3.0

*Publication date:*  
2020

*Document Version*  
Accepted author manuscript, peer reviewed version

[Link to publication from Aalborg University](#)

*Citation for published version (APA):*  
Garenfeld, M. A., Mortensen, C. K., Štrbac, M., Dideriksen, J. L., & Dosen, S. (2020). Amplitude versus spatially modulated electrotactile feedback for myoelectric control of two degrees of freedom. *Journal of Neural Engineering*, 17(4), Article 046034. Advance online publication. <https://doi.org/10.1088/1741-2552/aba4fd>

### General rights

Copyright and moral rights for the publications made accessible in the public portal are retained by the authors and/or other copyright owners and it is a condition of accessing publications that users recognise and abide by the legal requirements associated with these rights.

- Users may download and print one copy of any publication from the public portal for the purpose of private study or research.
- You may not further distribute the material or use it for any profit-making activity or commercial gain
- You may freely distribute the URL identifying the publication in the public portal -

### Take down policy

If you believe that this document breaches copyright please contact us at [vbn@aub.aau.dk](mailto:vbn@aub.aau.dk) providing details, and we will remove access to the work immediately and investigate your claim.

ACCEPTED MANUSCRIPT

## Amplitude versus spatially modulated electrotactile feedback for myoelectric control of two degrees of freedom

To cite this article before publication: Martin Alexander Garenfeld *et al* 2020 *J. Neural Eng.* in press <https://doi.org/10.1088/1741-2552/aba4fd>

### Manuscript version: Accepted Manuscript

Accepted Manuscript is “the version of the article accepted for publication including all changes made as a result of the peer review process, and which may also include the addition to the article by IOP Publishing of a header, an article ID, a cover sheet and/or an ‘Accepted Manuscript’ watermark, but excluding any other editing, typesetting or other changes made by IOP Publishing and/or its licensors”

This Accepted Manuscript is © 2020 IOP Publishing Ltd.

During the embargo period (the 12 month period from the publication of the Version of Record of this article), the Accepted Manuscript is fully protected by copyright and cannot be reused or reposted elsewhere.

As the Version of Record of this article is going to be / has been published on a subscription basis, this Accepted Manuscript is available for reuse under a CC BY-NC-ND 3.0 licence after the 12 month embargo period.

After the embargo period, everyone is permitted to use copy and redistribute this article for non-commercial purposes only, provided that they adhere to all the terms of the licence <https://creativecommons.org/licenses/by-nc-nd/3.0>

Although reasonable endeavours have been taken to obtain all necessary permissions from third parties to include their copyrighted content within this article, their full citation and copyright line may not be present in this Accepted Manuscript version. Before using any content from this article, please refer to the Version of Record on IOPscience once published for full citation and copyright details, as permissions will likely be required. All third party content is fully copyright protected, unless specifically stated otherwise in the figure caption in the Version of Record.

View the [article online](#) for updates and enhancements.

# Amplitude versus spatially modulated electrotactile feedback for myoelectric control of two degrees of freedom

Martin A. Garenfeld<sup>1</sup>, Christian K. Mortensen<sup>1</sup>, Matija Strbac<sup>2</sup>, Jakob L. Dideriksen<sup>1</sup> and Strahinja Dosen<sup>1</sup>

<sup>1</sup> Department of Health Science and Technology, Aalborg University, Frederik Bajers Vej 7D 9220 Aalborg Ø, Denmark

<sup>2</sup> Tecnalia Serbia Ltd., Deligradska 9/39 11000 Belgrade, Serbia

E-mail: [magar@hst.aau.dk](mailto:magar@hst.aau.dk) and [sdosen@hst.aau.dk](mailto:sdosen@hst.aau.dk)

Received xxxxxx

Accepted for publication xxxxxx

Published xxxxxx

## Abstract

*Objective.* Artificial proprioceptive feedback from a myoelectric prosthesis is an important aspect in enhancing embodiment and user satisfaction, possibly lowering the demand for visual attention while controlling a prosthesis in everyday tasks. Contemporary myoelectric prostheses are advanced mechatronic systems with multiple degrees of freedom, and therefore, to communicate the prosthesis state, the feedback interface needs to transmit several variables simultaneously. In the present study, two different configurations for conveying proprioceptive information of wrist rotation and hand aperture through multichannel electrotactile stimulation were developed and evaluated during online myoelectric control. *Approach.* Myoelectric recordings were acquired from the dominant forearm and electrotactile stimulation was delivered on the non-dominant forearm using a compact interface. The first feedback configuration, which was based on spatial coding, transmitted the information using a moving tactile stimulus, whereas the second, amplitude-based configuration conveyed the position via sensation intensity. Thirteen able-bodied subjects used pattern classification-based myoelectric control with both feedback configurations to accomplish a target-reaching task. *Main results.* High task performance (completion rate > 90%) was observed for both configurations, with no significant difference in completion rate, time to reach the target and path efficiency, respectively. *Significance.* Overall, the results demonstrated that both feedback configurations allowed subjects to perceive and interpret two feedback variables delivered simultaneously, despite using a compact stimulation interface. This is an encouraging result for the prospect of communicating the full state of a multifunctional hand prosthesis.

**Keywords:** Closed-loop control, electrotactile stimulation, myoelectric prosthesis, proprioceptive feedback, sensory feedback.

## 1. Introduction

The loss of an upper limb is a traumatic and life-changing event leading to a significantly reduced quality of life due to restrictions in function, sensation and appearance [1,2]. In an effort to restore normal functionality, myoelectric prostheses of various complexity have been introduced to replace the missing limb [3]. However, despite advancements in prosthetic technologies about 25% of users choose to abandon

their myoelectric prosthetic device [4]. In user reviews, different reasons for the low user satisfaction were listed, from limitations in ergonomics to problems in control robustness and dexterity [5]. The lack of exteroceptive and proprioceptive feedback is also often indicated as an important problem and future design goal [1,6], and may contribute indirectly to suboptimal control. Specifically, without somatosensory feedback, the user must rely only on visual observations when controlling the prosthesis, which is cognitively taxing [7].

Therefore, closing the loop is expected to improve prosthesis utility and user experience. Indeed, several studies have found that providing tactile stimulation through substitution feedback interfaces can improve user performance [8–12]. However, only one commercially available prosthesis (VINCENT evolution 2, Vincent Systems GmbH, Germany), provides the user with feedback information about grasping force using a single vibrotactile motor [13].

Some techniques for restoring somatosensory feedback can elicit somatotopic sensations; i.e., they are felt as emanating from the phantom limb, which presumably enables more intuitive interpretation [14]. Although this can be achieved to some degree via transcutaneous electrical nerve stimulation [15,16]. Such feedback is typically implemented by electrically stimulating peripheral sensory nerves [17,18] or somatosensory cortex in the brain [19,20] using implanted electrodes. Since this activates the same neural structures that have been used before amputation, the elicited sensations can be felt as emanating from the phantom limb. Some amputees, however, can be reluctant to undergo additional invasive treatments due to associated risks of post-surgery complications [5]. Alternatively, the feedback can be restored using a method called sensory substitution [14]. This is a non-invasive approach in which sensor data from the prosthesis are transmitted to the user by delivering mechanical or electrical stimulation to the skin of his/her residual limb.

The two most common substitution feedback methods are vibrotactile and electrotactile stimulation [21,22]. The former relies on miniature motors to generate vibrations that can be tangential or perpendicular to the skin, while the latter elicits tactile sensations by delivering low-intensity electrical pulses to activate skin afferents. Electrical stimulation can produce uncomfortable sensations if the parameters are not appropriately adjusted. However, it is also characterized by low power consumption, decoupled parameters, and compact electronics that can be customized in a wide range of configurations with different number and arrangement of electrode pads [23]. To deliver feedback information, the prosthesis sensor data has to be translated into stimulation profiles by associating the sensor information to stimulation parameters and location [24]. With parameter modulation, a feedback variable is communicated by changing stimulation intensity and/or frequency, while with spatial coding the variable is conveyed by changing active electrode pads [25].

In most studies in the literature, feedback interfaces were designed to transmit a single feedback variable, most often the grasping force [14,26]. Nevertheless, the users have also expressed an interest in receiving proprioceptive information [6]. The proprioceptive feedback is particularly important in the execution of movements without full visual attention [27]. Communicating proprioceptive information might lower the need for visual attention during prosthesis use, thereby decreasing the cognitive load [6]. Contrary to force feedback that was investigated in many studies (reviewed in [14,26]), artificial proprioception was addressed in only few works

using invasive [28,29] and non-invasive [30,31] methods.

Importantly, commercially available upper-limb prosthetic devices have multiple degrees of freedom (DoFs) [5]. A typical configuration is a gripper that can open and close equipped with a wrist rotation unit. Therefore, to provide full information regarding the state of this system, hand aperture as well as wrist rotation angle need to be transmitted simultaneously.

The studies investigating the communication of more feedback variables have used different tactile displays [9,10,28,32–34]. In [9] and [10], Witteveen *et al.* transmitted the sensory feedback of grasping force and hand aperture through a single vibrator and an array of vibrotactile actuators, respectively. Schiefer *et al.* [28] implemented the feedback of fingertip pressure and hand aperture delivered through peripheral nerve stimulation. Arakeri *et al.* [33] provided information regarding grip force and hand aperture by modulating the amplitude of two independent electrode pairs located on the dorsal left and right side of the neck. In [34], D’Anna *et al.* provided hand aperture and grip force information via amplitude modulated intraneural electrical stimulation.

Therefore, most of the previous studies relied on the parameter modulation via two stimulation channels to simultaneously communicate two feedback variables. The other coding schemes such as spatial modulation were not investigated (except in [9,10]) and more importantly, different encodings have not been compared in terms of effectiveness. The latter is particularly relevant considering that the compact solutions for multichannel tactile stimulation are becoming available (see [32]). Such systems, equipped with many channels and independently adjustable parameters, allow a great flexibility in designing stimulation patterns that can be modulated in time, parameter and space to communicate the feedback on multiple DoFs simultaneously.

In the present study, therefore, a compact electronic stimulator with 16 channels [32] was used to directly compare the performance of two novel stimulation schemes based on spatial and amplitude coding, respectively. The encodings were designed to convey simultaneous electrotactile proprioceptive feedback from two DoFs of a prosthesis, namely, wrist pronation/supination and hand aperture. In this case, the challenge is that the subject needs to independently perceive and interpret two electrotactile information channels that are delivered at the same time to the skin using a compact interface with closely spaced pads. The use of the simultaneous multi-DoF feedback was tested during online myoelectric control, which includes not only perception and interpretation of elicited sensations but also mapping of the feedback into appropriate command signals. The hypothesis was that the spatial modulation, communicating proprioceptive information by a moving stimulus, would

perform better than the amplitude encoding since the former might be more intuitive and easier to discriminate.

## 2. Methods

The two feedback schemes were evaluated by integrating the electrotactile interface into a commonly used setup [35–39] for the assessment of online myoelectric control based on pattern classification and target reaching task.

### 2.1 Experimental setup

The experimental setup is shown in *Fig. 1*. For the recording of electromyographic (EMG) signals, the Myo Armband from Thalmic Labs was placed on the dominant forearm, approximately 5 cm distally from the elbow crease with the main module (signed with the logo) positioned in the middle of the dorsal side. The Myo Armband integrates eight dry, stainless-steel electrode channels that are equidistantly arranged around the circumference of the forearm. The armband was connected via a Bluetooth 4.0 unit to a standard desktop PC. Despite having a limited sample rate of 200 Hz, high classification accuracy for myoelectric control can be achieved [40]. This configuration of EMG electrodes has been commonly used for myoelectric control [41].

The electrode array used to deliver electrical stimulation is shown in *Fig. 2*. The electrode array consisted of a single

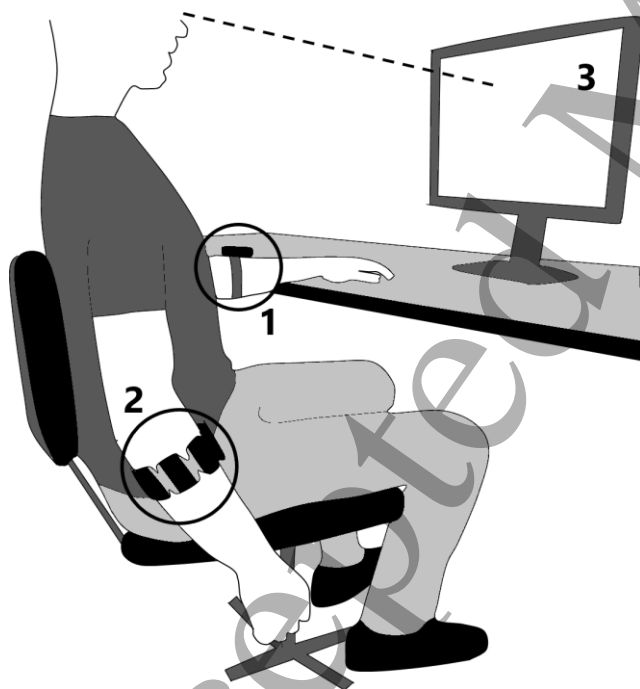


*Fig. 1.* Illustration of the experimental setup: 1) the stimulation system with the electrode array (see *Fig 2*) wrapped circumferentially around the non-dominant forearm and a stimulator placed on the dorsal side connected to a computer via USB; 2) the Myo armband placed on the dominant forearm to record EMG; and 3) the computer screen displaying the tasks to be performed in the experiment.

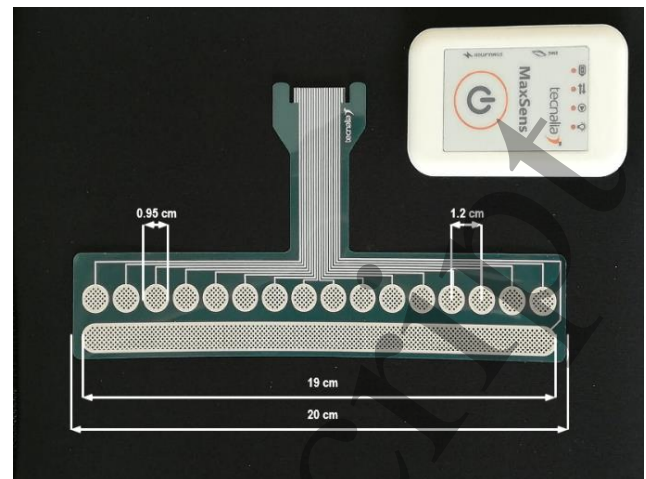


*Fig. 2.* The 16-pad electrode array and the MaxSens stimulator. The electrode consisted of 16 circular active pads and a common reference pad.

elongated pad designated as a common reference electrode and 16 circular pads designated to act as active electrodes. The electrodes were made by screen-printing conductive Ag/AgCl and dielectric inks for biomedical applications over 150  $\mu\text{m}$  thick PET film. All pads were covered with conductive hydrogel (AG725, Axelgaard, Denmark) to enhance skin-electrode contact. A compact multichannel stimulation device (MaxSens, Tecnia, Spain) generating biphasic pulses was connected to the standard desktop PC via USB. The pulse width and amplitude could be modulated independently for each pad whereas the frequency was common to all pads. The pulse width could be adjusted within a 50 - 1000  $\mu\text{s}$  range with 10  $\mu\text{s}$  steps, frequency from 1 - 400 Hz with 1 Hz steps and current amplitude from 50 - 10000  $\mu\text{A}$  with 0.1  $\mu\text{A}$  steps. The electrode array was indeed designed to provide feedback on the forearm [25,32,42], and it can be placed either longitudinally or transversely. A recent study has shown that there was no substantial difference between the two arrangements [43], and therefore, the circumferential placement was selected in the present setup because it is more compact. The electrode was wrapped around the non-dominant arm of the participant (*Fig. 1*) to avoid contaminating the recorded EMG [44,45]. It was fitted such that the end pads had a maximum gap of 3 cm centrally on the volar side. Hence, the distal location of the electrode array depended on the circumference of the subject's forearm. This positioning strategy was applied to assure that the electrode covered as much of the circumference as possible. Therefore, the stimulation could be delivered to both sides of the arm with no spatial overlap between the most distal pads. The electrode connector (*Fig. 2*) was aligned with the axis of the forearm and positioned along the middle of the dorsal side. The electrode was strapped by an elastic sport band and the stimulator was attached to the top of the band (*Fig. 1*).

The subject was seated in a comfortable chair. During the experiment, the non-dominant hand was placed on the table and the dominant hand was held vertically relaxed by the side

of the body. A 22" monitor was positioned on the table approximately 50 cm from the subject. The monitor was used to provide visual feedback when required (see 2.4. *Experimental protocol*). The desktop PC received recorded EMG and controlled stimulation parameters. The online control loop was programmed in Matlab 2018b (MathWorks, USA).

## 2.2 Myoelectric control

The movement classes used for myoelectric control were wrist supination and pronation, opening and closing of the hand and rest. These DoFs were selected since they can provide control of wrist rotation and hand aperture in a myoelectric prosthesis. The acquired EMG signals were filtered using a 2<sup>nd</sup> order Butterworth high-pass filter with 10 Hz cut-off to remove movement artefacts. For feature representation spatial features designed by Donovan *et al.* [46], namely, scaled mean absolute value, correlation coefficient, normalized mean absolute difference, and scaled raw mean absolute difference, were extracted along with the waveform length, hence 5 features per channel [47]. The features were extracted in windows of 200 ms with a 50% overlap to obtain fast update time, while preserving good classification accuracy [48].

Training data were acquired by asking the subjects to track a trapezoidal trajectory comprised of 3-s incline time, 5-s plateau and 3-s decline. The cursor moved horizontally with time while the vertical position was adjusted by the subject's contraction intensity. The plateaus of the trapezoidal profiles were at 40%, 50% and 70% of a prolonged maximum voluntary contraction (15 s). The three trajectories were tracked by the subjects for each movement class [49]. A 15-s recording of rest was acquired at the end.

The extracted features were used to train a sequential proportional control system. For sequential control, a linear discriminant analysis (LDA) classifier was trained and for proportional control, multiple linear regression models were used, one per movement class. This configuration was chosen because it is commonly applied for myoelectric control in the literature [50–55]. The LDA classifier can be trained fast, while still yielding robust control [52]. Linear discriminant analysis models the feature distribution within each class using a Gaussian distribution, assuming that all classes share the same covariance matrix. To classify a test sample, the posterior probabilities are computed by using Bayes' rule, and the class with the highest posterior probability is the output of the classifier, as explained in [56]. The multiple linear regression model fitted for the decided movement class provided the proportional control output. The input of the regression model was a vector of mean absolute values calculated from a single window in each EMG channel. The output was the normalized level of muscle activation within the selected movement class.

The control of a two-DoF prosthesis was simulated by a

planar cursor control task similarly to previous work [35]. The output of the myoelectric controller was a recognized movement class and a normalized value of the intensity of muscle contraction. The detected class determined the movement direction of the cursor (*Fig. 3*). Performing supination, pronation, opening and closing moved the cursor to the right, left, upwards, and downwards along the plane, respectively, while the estimated contraction intensity was mapped to the velocity of cursor movement. The cursor was controlled in velocity since this approach is used with commercial prostheses [57], where the muscle activation of the user is mapped into the velocity of prosthesis movement. The cursor initial position, as indicated in *Fig. 3*, represented a neutral prosthesis state, i.e., hand horizontal and fully open. Then, left and right movements of the cursor simulated wrist rotation into pronation and supination, while downwards and upwards movements corresponded to a decrease and increase in hand aperture, respectively. The maximum velocity of the cursor was adjusted so that a full range of each DoF could be traversed in 2 seconds. This corresponds to a maximum velocity of opening and closing in a Bebionic (RSL Steeper, United Kingdom) prosthesis [58]. The cursor moved smoothly within the plane; however, the plane was divided by a grid to indicate that the electrotactile feedback on the cursor position was in fact discrete, as explained in 2.3. Each field of the grid corresponded to a unique combination of levels of wrist rotation and hand aperture.

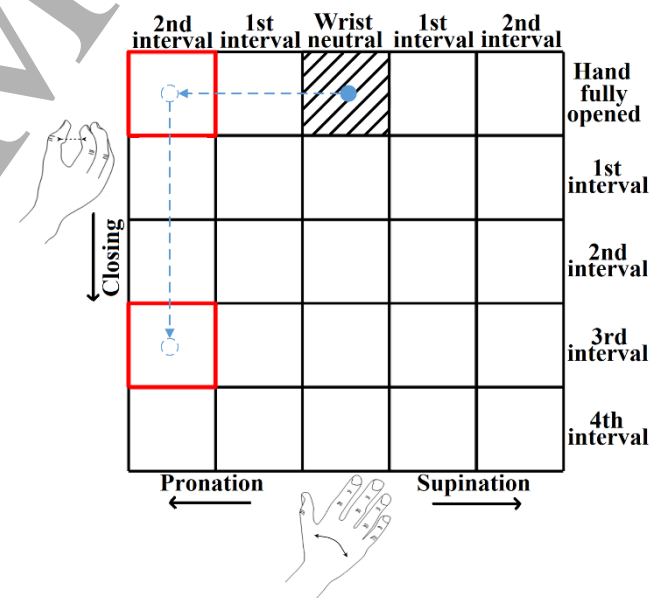


Fig. 3. Illustration of the grid for the planar cursor control task and an example of two target cells. For the cursor (blue circle) to reach the target cell in first row and first column, a pronation must be performed, and to reach the one in fourth row and first column, a pronation followed by a decrease in hand aperture must be performed. The striped grid cell indicates a neutral position, i.e., a prosthesis, which is fully opened and with the palm in a horizontal position.

## 2.3 Feedback configurations

Two coding schemes were designed to transmit wrist rotation and hand aperture information. As in previous studies a discrete coding strategy was adopted for both schemes [7,32,44,59,60]. Specifically, the full range of each feedback variable was divided into five segments, as shown in *Fig. 3*.

### 2.3.1 Spatial configuration.

This feedback design was chosen in order to be intuitive for the subject, similar to what was initially proposed in [32]. The two proprioceptive feedback variables were coded by a spatially moving electro-tactile stimulus. In addition, the movement of the stimulus mimicked the directions of the motion in the included DoFs. Wrist rotation was communicated by producing a stimulus that rotated around the forearm. Hand aperture was transmitted by moving two pads closer together as the hand closed and further apart during hand opening. The illustration of the spatial configuration can be seen in *Fig. 4d*.

The pads were divided into two groups each responsible for conveying information about a single DoF. The dorsally placed pads were allocated for wrist rotation and the volar pads for hand aperture. The pads were furthermore paired such that each pair would represent one of the four intervals of the proprioceptive feedback variable. The absence of stimulation in all pad groups indicated the first interval, hence five in total. For wrist rotation, the pads were connected in side-by-side pairs. For right-handed subjects, the activation of the pairs of pads would rotate laterally during supination and medially during pronation. For hand aperture, the pairs consisted of oppositely located pads on the medial and lateral sides. When decreasing hand aperture, the active pads would move towards the volar side of the forearm and the distance between the pads would become shorter, and opposite for the increase. When both feedback variables were outside of the first interval (no stimulation), the pad pairs corresponding to the given level of hand aperture and rotation would be activated. Thus, a maximum of four pads could be active simultaneously. The reason for grouping adjacent pads to convey information about

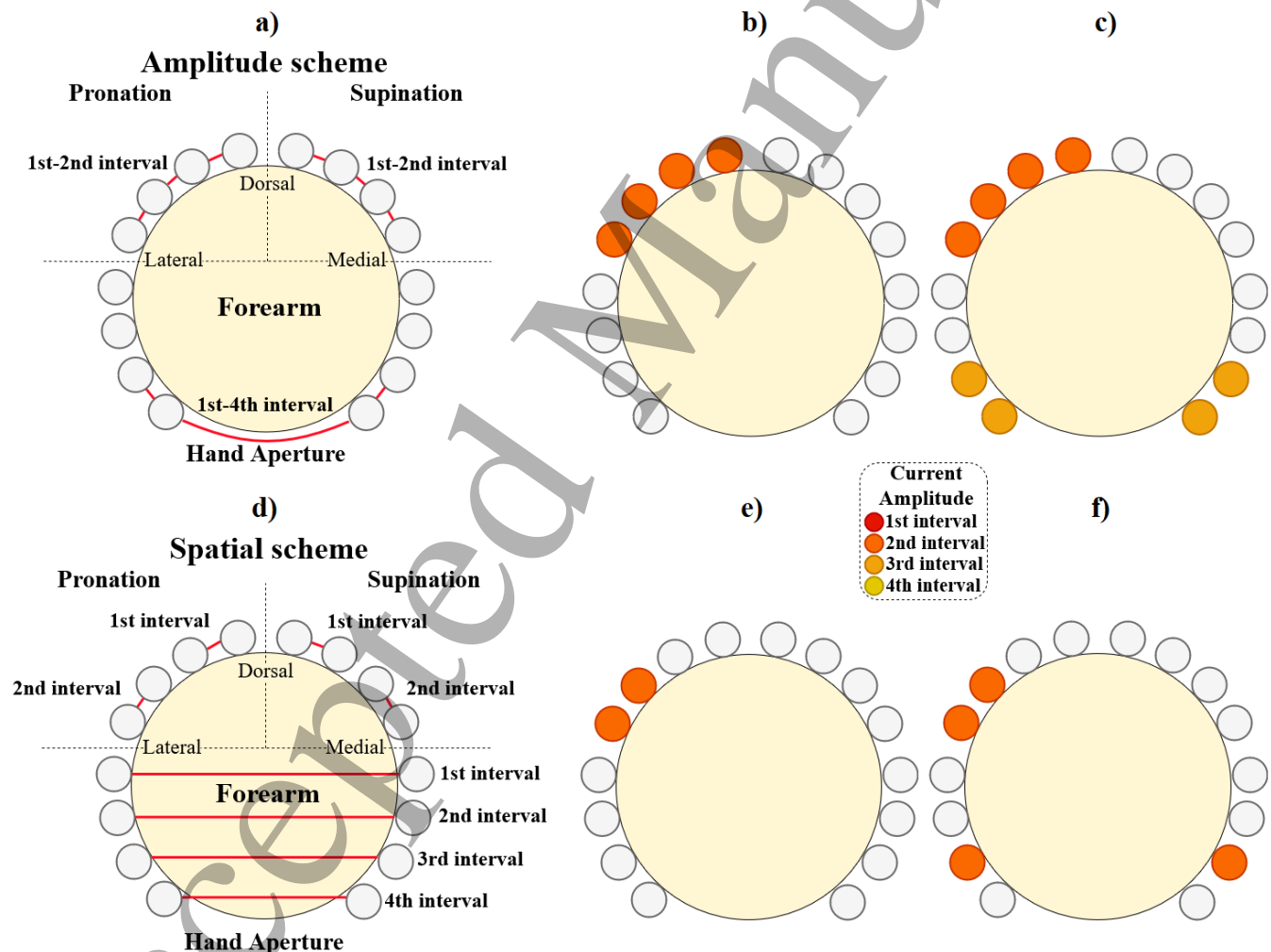


Fig. 4. Illustration of the feedback schemes, **a)** shows the amplitude coding and **d)** shows the spatial coding. The red lines indicate which pads were coupled (see text). For the amplitude coding, the stimulation amplitude represented the position interval, whereas with spatial coding the position interval was communicated through location of active pads. The stimulation illustrated in **b)** and **e)** correspond to the position interval of the upper target cell in *Fig. 3*., for the amplitude and spatial coding, respectively, where **c)** and **f)** correspond to the lower target cell in *Fig. 3*.

the rotational DoF was to improve sensation perception by stimulating a larger skin area, as in [25].

### 2.3.2 Amplitude configuration.

This is a simple coding scheme, in which the proprioceptive information is conveyed by increasing the current pulse amplitude. The advantage of this approach is that even more pads can be grouped together to stimulate a larger area of the skin, thereby eliciting clearer sensations. The feedback was provided in groups of four pads. An illustration of the amplitude-coding scheme can be seen in *Fig. 4a*.

The dorsal area of the electrode was associated to wrist rotation and the volar to hand aperture, as in the spatial coding scheme. However, in the amplitude scheme, the decrease in the hand aperture was communicated by simultaneously increasing the pulse amplitude of the 4 volar pads through 4 levels plus no stimulation, hence 5 levels in total. The eight pads used for the wrist rotation were split such that the four laterally placed pads communicated supination and four medially placed indicated pronation. The amplitude of both groups could be changed through 2 levels, hence 5 levels in total, i.e., 2 pad groups times 2 levels plus no stimulation. The increasing amplitude corresponded to increased rotation in the respective direction. Since both DoFs were transmitted simultaneously, a maximum of eight pads could be active concurrently.

### 2.4. Experimental protocol

Thirteen able-bodied subjects (12 males and 1 female - 12 right-handed and 1 left-handed with a mean age of  $26.3 \pm 2.3$  years) were recruited. The subjects signed an informed consent form before commencing with the experiment. The experimental protocol was approved by the ethical committee of Region Nordjylland, Denmark (approval number N-20150075).

Each subject was introduced to each feedback configuration, trained to perceive and interpret the feedback, and finally performed an online myoelectric control task. The order of the feedback schemes was randomized across subjects. The duration of the experiment was approximately 2.5 hours.

First, the electro tactile and EMG recording systems were placed on the subject, as explained in 2.1. Then, the training data for the myoelectric controller were collected, as described in 2.2. Next, the subject practiced controlling the cursor movement using the myoelectric interface and visual feedback. It was crucial for the subject to achieve effective control since poor control could mask potential differences in performance between feedback configurations. The quality of closed-loop control was assessed by employing a target reaching task, which is a commonly used experimental paradigm to evaluate online myoelectric control [35–39]. The subject was presented with a grid shown in *Fig. 3*. The cursor

was in the initial position. The subject training was divided into two runs of three minutes with a different visual feedback in each run. In the first run, the subject moved the cursor continuously and the current cursor position was shown on the screen. In the second run, the subject still moved the cursor in a continuous way; however, the visual feedback indicated only the cell of the grid currently containing the cursor. Therefore, the discretized visual feedback transmitted the same information as the electro tactile feedback that would be used later in the session.

After this brief training, the subject performed the target-reaching test using a discretized visual feedback. The task for the subject was to move the cursor from the initial position to the highlighted target position (grid cell highlighted in red) and dwell in that position for 1.5 s. The subject had 30 s to reach the target. This time was selected through pilot tests. The aim was to provide enough time so that the subjects were not pressured by the timer while still limiting the total duration of the experiment, as well as mental and physical fatigue due to continuous control. If the target was reached successfully, or the time limit expired (trial unsuccessful), the cursor would reset to neutral position and a new trial began. The grid cells were selected as targets in a random order and the test was finished when all the grid cells had been highlighted, hence 24 targets. If the subject did not achieve a completion rate  $> 90\%$  and a mean time to reach the target  $< 10$  s, the control was deemed ineffective and the subject was excluded. To reach the cells in the first row and third column (hereafter, single DoF targets), the subject would ideally move along a single DoF, and for the other cells, the subject needed to adjust both DoFs (hereafter, combined DoFs targets).

Next, four distinguishable stimulation levels were determined for each electrode pad. The stimulation levels were determined by changing amplitude while the pulse width and frequency were constant and set to 500  $\mu$ s and 50 Hz, respectively.

To determine the stimulation levels the ascending method of limits [61] was applied to assess the sensation and discomfort thresholds. For the sensation threshold, the amplitude was set to 0  $\mu$ A and increased in steps of 100  $\mu$ A until the subject reported that he/she felt the sensation. For the discomfort threshold, the amplitude was initialized at the sensation threshold and increased in steps of 200  $\mu$ A until the subject reported the stimulation as uncomfortable. First, the sensation thresholds were determined for all pads and then the amplitude values were fine-tuned by comparing the sensation intensity in neighboring pads. The goal was to achieve similar sensations across pads. The resulting amplitude was adopted as the first stimulation level. The same was then done for the discomfort threshold, and the resulting amplitude was adopted as the fourth stimulation level. The second and third stimulation levels were determined as the points that equidistantly divide the range between the first and fourth level.

In the spatial-coding scheme, all electrode pads were

1  
2  
3 activated at the second level of stimulation intensity. The  
4 second intensity level was used to ensure that the stimulation  
5 elicits a sensation that could be clearly perceived by the  
6 subjects. This intensity was well above the detection threshold  
7 and still below the discomfort threshold. In the amplitude-  
8 coding scheme, the aperture pad group was activated at all  
9 four intensity levels, and the two wrist rotation groups were  
10 activated at the second and third level of stimulation intensity.

11 Following the psychometrics test, the subject was trained in  
12 understanding the sensory feedback schemes. The feedback  
13 schemes were first explained to the subject verbally. The  
14 sensory feedback training was divided into two phases:  
15 familiarization and reinforced learning. The familiarization  
16 phase provided the subjects with a short introduction to the  
17 scheme. The cursor was visualized and moved by the  
18 investigator from the neutral position to a designated target  
19 cell. At the same time, the subject received electro-tactile  
20 feedback on the cursor position. Therefore, the subject could  
21 associate visual feedback (the currently highlighted grid cell)  
22 to the electro-tactile feedback that is being delivered. The  
23 experimenter visited the grid cells along the row and column  
24 containing the neutral state, which corresponded to moving  
25 along a single DoF. This was deemed most important, since it  
26 was assumed that the subject will be able to recognize  
27 simultaneous feedback if he/she understands each DoF  
28 individually.

29 In the reinforced learning phase, the subject was asked to  
30 look away from the screen. The experimenter moved the  
31 cursor to a designated target cell and the subject was asked to  
32 report the grid cell solely by focusing on the electro-tactile  
33 feedback. If the subject answered correctly, the cursor was  
34 reset to the neutral position and then moved to a new grid cell.  
35 If the subject answered incorrectly, the experimenter would  
36 indicate the correct cell verbally. Every cell of the grid was  
37 presented as the target once by moving the cursor along the  
38 optimal path (the cursor was moved fully in one DoF and then  
39 in the other). However, the order of the DoFs was varied to  
40 avoid biasing the subject. When all 24 cells were trained, the  
41 subject was given a short break before repeating the reinforced  
42 learning. The order of the target cells and DoFs was changed  
43 in the second run. The subject was given two minutes rest  
44 between the runs to avoid sensory adaptation.

45 Until this point, the subject trained the cursor control and  
46 sensory feedback separately. Both components were finally  
47 combined in the last phase of the experimental session, where  
48 online closed-loop control was assessed.

49 The subject was given a three-minute training period to be  
50 reacquainted with the myoelectric control and to further train  
51 the understanding of the feedback scheme. After a two  
52 minutes break, the subject performed a target-reaching test  
53 identical to that used with the visual feedback at the beginning  
54 of the session (target cell indicated by red color). However,  
55 this time the visual feedback on the cursor position was  
56 removed. Therefore, the subject had to estimate the cursor  
57 position solely by relying on the electro-tactile feedback. The

target-reaching test was performed two times with all cells of  
the grid as targets (24 repetitions) and there were two minutes  
of rest in between the two tests.

In order to preliminary assess the subjects' preference  
regarding the coding schemes, they were asked two questions  
at the end of the experiment: 1) whether they found the coding  
schemes intuitive to understand, and 2) which coding scheme,  
amplitude or spatial, they favored (if any).

### 2.5. Data analysis

The outcome measures were the number of successfully  
reached targets expressed in percent (completion rate), time to  
reach the target and path efficiency. These measures are  
commonly used in literature to evaluate the quality of control  
in target reaching tasks [35,36]. Ideally, the subjects would be  
able to employ the closed-loop interface (myoelectric control  
and electro-tactile feedback) to navigate the cursor from the  
initial to the target cell (configure the prosthesis DoFs) in  
minimum time and using the shortest path. Importantly, only  
successful trials were considered when computing the time to  
reach the target and path efficiency. Unsuccessful trials in  
which the 30-s timer has expired before the target was reached  
were excluded from this analysis. They were instead used to  
compute the distance error. The time to reach the target was  
measured from the start of a successful trial until the target  
was reached, including the dwell time. Path efficiency was  
computed by dividing the length of the shortest path from the  
initial position to the target with the length of the path that  
was actually traversed during online control. For single DoF  
targets, the shortest path was the distance in a straight line  
from the initial position to the border of the target, and for  
combined DoF targets, it was the distance to the target corner  
closest to the initial position. The distance error was calculated  
as the number of grid cells between the cursor and the target  
cell at the end of a trial. For instance, if the cursor was inside  
the target when surpassing the time limit, the distance was 0.  
If the cursor reached an adjacent grid cell directly above,  
below, left or right from the target, the distance was set to 1,  
and if the cursor ended up in an adjacent cell placed diagonally  
to the target, the distance was set to 2. This considered that the  
myoelectric control was sequential and the subjects could  
therefore move only in horizontal and vertical direction,  
hence, two cells would need to be traversed before reaching  
the target. The maximum score would then be 8, if the end-  
point was e.g. in the top-left grid cell when the target was the  
bottom right grid cell. The outcome measures were computed  
for each trial and then averaged across all trials of a single  
subject in each feedback condition. The outcome measures  
computed for the online control with the visual feedback were  
used as the benchmark. Since the data were not normally  
distributed based on one-sample Kolmogorov-Smirnov tests,  
comparisons were made using non-parametric statistics. For  
the completion rate, time to reach the target and path  
efficiency, the Friedman test was used to assess if there was a

statistically significant difference between the feedback modalities, and Tukey’s honestly significant difference test was used for post-hoc pairwise comparisons. As the control with the visual feedback resulted in only three unsuccessful trials overall, the distance error was not evaluated in this condition. The distance error achieved with the spatial and amplitude feedback was compared using Wilcoxon signed-rank test. A significance level was set at  $p < 0.05$ . The results in the text are reported as median{interquartile range (IQR)}.

### 3. Results

#### 3.1. Representative trajectories

Fig. 5. shows examples of trajectories generated by subjects using spatial feedback to reach a target (red square) corresponding to the combined movement along both DoFs.

The cyan dashed lines demonstrate very good performances, while the blue dashed line is an example of a detour from the ideal path. The former trajectories indicate that the subjects successfully used the feedback to reach the target via a short route, i.e., the sequential movements along both DoFs were of appropriate magnitude. The two traces illustrate that the subjects could chose to move along the DoFs in a different order, that is, first adjust wrist rotation and then hand aperture, or vice versa. In this example, the subjects achieved a high performance in both cases, namely, a completion time of 7 s and 5.5 s, respectively, and a path efficiency of 74% and 70%, respectively. In the example with a detour, however, the subject misinterpreted the hand aperture interval before performing supination. When reaching the correct supination interval, the subject moved to a lower hand aperture before realizing the error and moving to the correct aperture. Therefore, the subject utilized the feedback to detect an erroneous level of a feedback variable

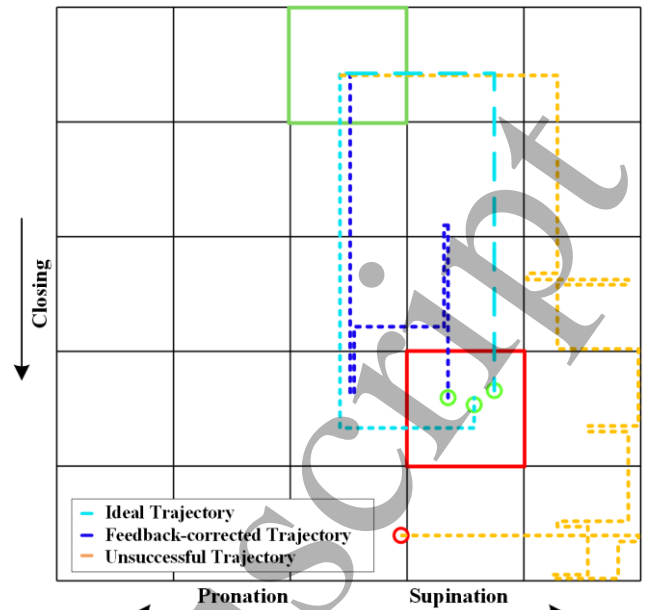


Fig. 5. Examples of prosthesis trajectories when reaching a combined DoF target (red box) in the target-reaching test. The black circle and red box indicate the starting point and target cell, respectively. The cyan dashed lines are examples of very good performance and the blue dashed line is a trajectory with several feedback-driven corrections. The orange trajectory is an example of an unsuccessful attempt at reaching the target. The green and red circles are end positions, indicating whether a particular trial was successful or not, respectively.

and correct the cursor position accordingly. In this case, the completion time was 16 s and the path efficiency 46%. The orange dashed line demonstrates an unsuccessful trial. The subject initially overshoot the target supination interval and then moved into higher hand aperture intervals. Finally, he/she moved towards the correct supination but did not successfully correct the hand aperture, thereby failing to reach the target (30-s timer expired). In this example, the path efficiency was

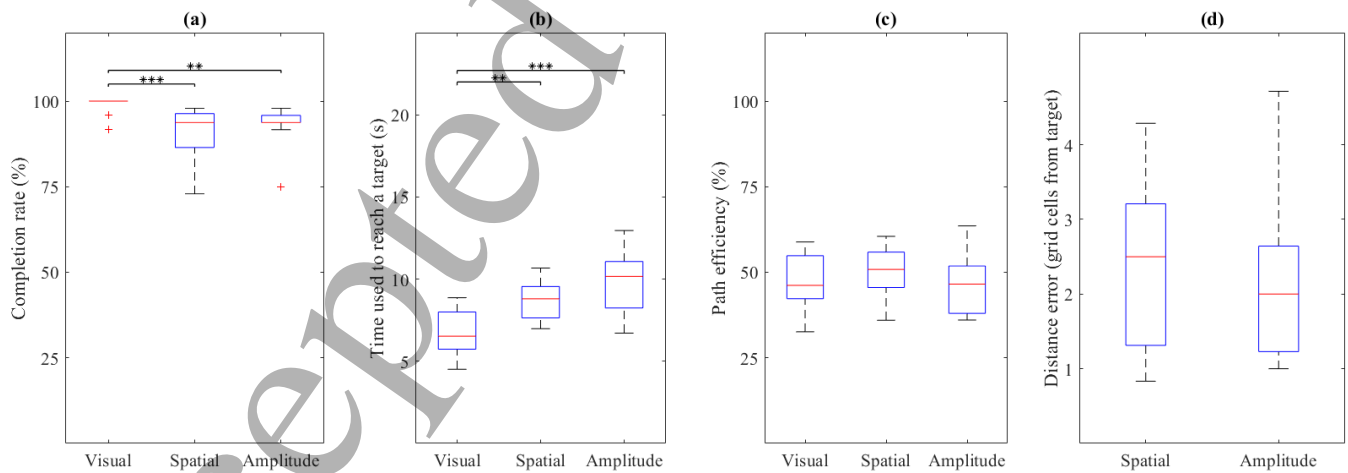


Fig. 6. Box plots of the outcome measures extracted from the target-reaching tests using visual, spatial and amplitude feedback: **a)** the completion rate, **b)** the time used to reach a target, **c)** the path efficiency and **d)** the distance error. The red line, blue box, and black whiskers indicate the median, interquartile range and maximum and minimum values, while the red crosses are outliers. The asterisks indicate a p-value (\*,  $p < 0.05$ ; \*\*,  $p < 0.01$ ; \*\*\*,  $p < 0.001$ ).

20% and the distance error was 2 cells.

### 3.2. Summary outcome measures

The success rate (median{IQR}) in estimating the grid cell using electro tactile feedback in the reinforced learning phase was 75{22}% and 79{14}% using spatial and amplitude coding, respectively, with no significant difference between the two feedback schemes. The summary results for the quality of online control using three feedback modalities are shown in Fig. 6. Overall, only 7% of trials were unsuccessful. The median completion rate for the amplitude coding was not significantly different to that of the spatial coding. Importantly, the performance was high with both feedback configurations, with the median completion rates of more than 90% (94{10}% for spatial and 94{2}% for amplitude coding). Similarly, no significant difference was found in the time to reach the target (9{2} s for spatial and 10{3} s for amplitude), path efficiency (51{10}% for spatial and 47{14}% for amplitude) and in distance error (2.5{1.9} grid cells from target for spatial and 2{1.4} grid cells from target for amplitude). Nevertheless, the mean completion rate and the time to reach the target were less variable across subjects when using amplitude coding. The amplitude condition was favored by 8 out of 13 subjects. However, most subjects struggled in choosing a favored feedback scheme as they found that both configurations were intuitive to understand. Accordingly, there was little difference in the completion rates across the preferred and non-preferred scheme (subjects preferring amplitude coding: 94{14}% for spatial and 94{3}% for amplitude; subjects preferring spatial coding: 90{9}% for spatial and 96{7}% for amplitude). As expected, the visual feedback outperformed both electro tactile feedback schemes. Almost all subjects reached all targets when using visual feedback and they were substantially faster (approximately

3.5 s per target) compared to online control with electro tactile feedback. Interestingly, the path efficiency for electro tactile feedback was similar to that of the visual feedback.

### 3.3. Completion rates for individual targets

Fig. 7. shows the completion rate for all targets individually. In both feedback schemes, the subjects were more successful in reaching the peripheral targets located along the edges of the grid, i.e., first and last row and column. In these targets, one or even both (corner cells) of the DoFs are close to the limits of their range of motion, and this includes both single-DoF targets (first row cells, bottom cell in the third column) and the combined-DoFs targets (all other peripheral cells). And indeed, the completion rate (median{IQR}) for the non-peripheral targets was 80{11}% with spatial feedback and 89{5}% with amplitude feedback, whereas the median completion rate for the peripheral targets was 96{2}% with spatial feedback and 96{7}% with amplitude feedback. The likely reason is that in the peripheral targets, the unintended myoelectric commands would not move the cursor outside of the cell due to the limits in the range of motion (as in a real prosthesis). Therefore, the subjects did not need to achieve an ideal rest state, while in the non-peripheral targets an unstable rest could lead to a cursor drifting outside of the cell during the dwell time. In addition, to reach a peripheral target, the subjects could rely on a simple control strategy where they would simply saturate the DoF in the direction of the peripheral cell.

The same reason is likely responsible for the fact that in both schemes a higher completion rate was achieved for the rotational single DoF targets (98{4}% with spatial and 98{6}% with amplitude coding) compared to the hand aperture single DoF targets (90{15}% for spatial and 90{8}% with amplitude coding). While moving along rotational DoF

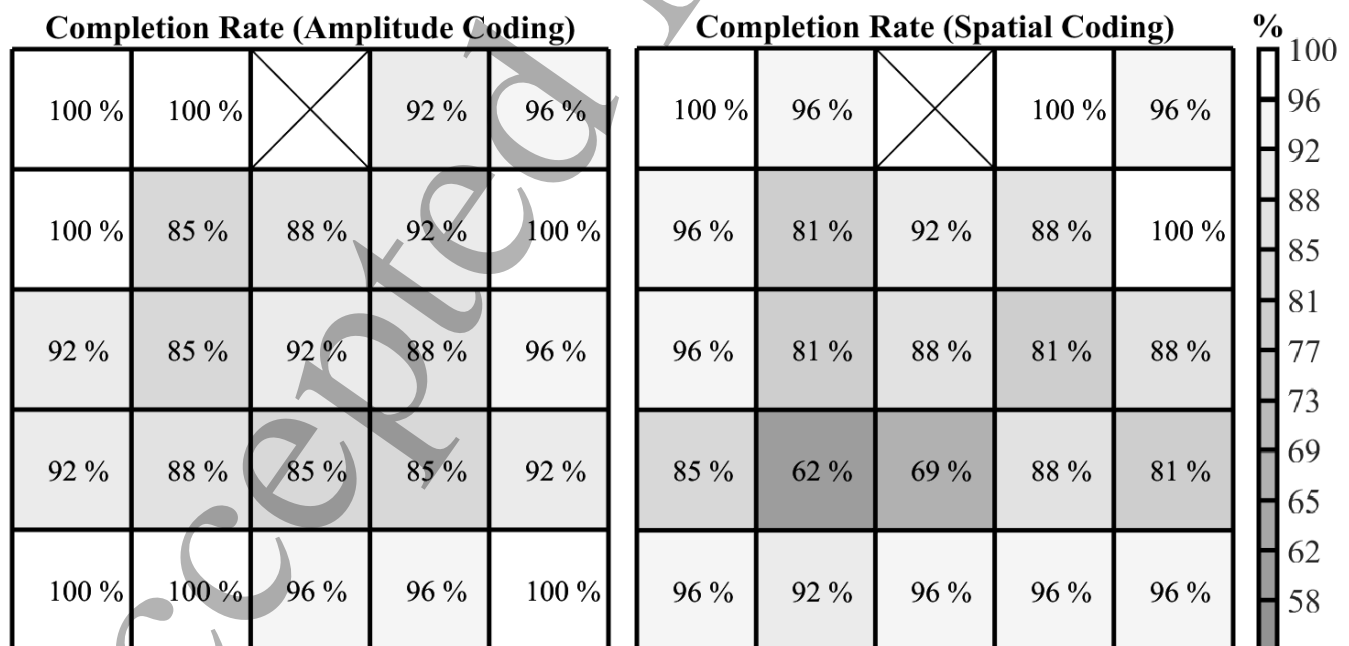


Fig. 7. Completion rate for each target in the target-reaching tests using the amplitude and spatial coding, respectively.

(first row), the hand aperture DoF is at the limit of the range of motion (the “hand” is fully open), whereas while closing the hand (third column), the wrist can be rotated both to the left and to the right.

The overall lowest completion rate (a cell with 62%) for spatial coding was worse compared to those of the amplitude coding (a cell with 85%).

#### 4. Discussion

A compact multichannel electro tactile system was used to develop two electro tactile feedback schemes using spatial and amplitude coding to provide proprioceptive feedback about two DoFs simultaneously. The schemes were tested in able-bodied subjects using sequential proportional myoelectric control to perform a target-reaching task with a velocity-controlled cursor (simulating prosthesis operation). A discrete electro tactile feedback provided 9 intervals along single DoFs and 16 combinations of intervals along two DoFs.

The results demonstrated that a very good performance was achieved with both feedback-coding schemes. The average completion rates were high and the path efficiency in the electro tactile conditions was not significantly different to that achieved with visual feedback (benchmark). Even when the subjects were not able to navigate successfully to the target cell, they still ended up in the vicinity of the target (median distance error  $\sim 2$  cells out of max distance of 8 cells). The subjects were therefore able to correctly perceive and interpret two independent channels of electro tactile stimulation, despite they were delivered simultaneously and through a compact interface with closely spaced pads. In addition, the patterns of stimulation were substantially different between the two schemes (amplitude change versus movement across the skin), but nevertheless, the subjects could exploit both configurations successfully during the online control.

Our initial hypothesis was that spatial coding would lead to better performance and user experience, since it was assumed that this was a more intuitive interface, in which the movement of the electro tactile stimuli mimicked the movement of the controlled object (cursor/prosthesis). However, both feedback schemes resulted in similar performance in both the evaluation test and reinforced learning with a slight advantage of amplitude coding, which was characterized with less variability across subjects. Strictly speaking, the amplitude scheme also included a spatial code as the pronation and supination were communicated through separate pad groups. This had to be done so that the neutral position could be communicated as no stimulation. This could have contributed to a better consistency of the amplitude scheme across subjects.

The present study further emphasizes the advantage of a flexible system for electro tactile stimulation that is capable of implementing different coding schemes. A prospective user could test both amplitude and spatial modulation and select the scheme that feels better. In addition, some users might have a low tolerance to stimulation intensity (low dynamic range) and in this case, spatial modulation would be the only option.

A similar coding scheme could be implemented using frequency instead of amplitude coding, but this could not be included in the present study due to technical constraints (frequency is a parameter common to all channels). An advantage of a flexible stimulation system is that it could be adjusted not only to the preference of the user but also to the characteristics of a specific prosthesis (multifunction versus dexterous device) or to the demands of a specific application (e.g., feedback in a lower limb prosthesis).

Importantly, the good performance in the present experiment was obtained after only a short training protocol (training time per scheme  $< 30$  minutes). It is likely that a longer training would lead to even higher completion rates, approaching the benchmark of visual feedback. The importance of training for the interpretation of tactile feedback has been demonstrated in [32] and [62]. However, as stated in [63], vision is dominant in learning motor control, and an equal performance should, therefore, not be expected.

An additional important conclusion from the present study is that the performance of closed-loop control is not determined only by the feedforward and feedback method, but also by the limitation and “mechanical” interaction between the DoFs. The subjects were better in reaching states in which one of the DoFs was at the limit of the range of motion, and this benefited wrist rotation more than hand aperture. Importantly, the times to reach the target were always well below the limit of 30 s, and this includes the pads with lower success rates placed centrally in the grid. Therefore, in the unsuccessful trials, the subjects likely failed not because they could not navigate to the correct pad (generate proper commands) but because they had difficulties to locate the pad by interpreting the feedback. In particular, two pads seemed to have been more challenging to find using spatial coding (Fig. 7, 62% and 69% success rates).

In general, it was a challenge to achieve a homogenous sensation during multi-site stimulation. This was especially apparent in the spatial scheme, where the sensation intensity was adjusted so that the elicited sensation was approximately identical in all pads. Some subjects reported difficulties in separating feedback variable levels, due to a notable difference in sensation intensity between them. The variation in the sensation intensity caused some feedback variable levels to be “washed out” when receiving information regarding two DoFs simultaneously, as a stronger sensation would mask the weaker one. Allocating more time for the psychophysics stage of the experiment might have resulted in better discriminability between the levels. This was not possible in the present experiment due to time constraints, but it will be possible in the prospective clinical applications. A recent study has proposed a promising approach to decrease the time needed for the calibration of stimulation parameters [64].

One limitation of the study was that the stimulation electrodes were positioned on the contralateral arm with respect to the EMG recording. Even if this affected the closed-

loop performance, which is unlikely, this is not relevant for the present study since the aim was to compare the relative performance of the two feedback schemes under the same conditions. Nevertheless, combining recording and stimulation into one device is required for clinical applications. Methods to minimize the interference have been proposed, such as, the use of concentric electrodes to minimize current leakage, time-division multiplexing [65], or artifact blanking and data segmentation [66]. Another limitation is the lack of amputee subjects and the fact that the myoelectric control did not involve a physical prosthesis. This, however, is unlikely to have affected the main outcome of the project, which was the comparison of two different coding schemes via a compact stimulation system during closed-loop control. Specifically, an amputee subject might find it more difficult to accurately perceive the stimulation [32,67], but this would likely affect both coding schemes in the same way. On the other hand, the presence of natural proprioception in the able-bodied subjects used in the study is unlikely to have provided an advantage in the test, since the cursor position was velocity-controlled and therefore could not be derived from wrist motions in a trivial way. Replacing the virtual interface (Fig. 3) with a real prosthesis would have introduced a movement delay, but this would also likely affect both coding schemes similarly. The next step in this research would be to investigate the performance while increasing the resolution of the feedback scheme. The number of levels with the spatial feedback could be increased if the pads would be taken individually and not in pairs. With the amplitude feedback, more intensity levels could be considered in each group of pads. In this case, the device restrictions and subjects' sensory discrimination abilities are the only limit to the feedback resolution. Recognizing more levels would be more challenging for the subjects, especially during combined DoFs control. Therefore, a longer training would likely be necessary. Importantly, continuous feedback or a higher number of feedback intervals might not be more beneficial during daily life tasks as high precision is often not necessary to accomplish functional tasks [59]. In addition, even though the feedback is discrete, the subjects could rely on internal models [68,69] and/or incidental feedback [70] to estimate the levels in-between those which are explicitly provided by the feedback.

The psychometric properties of electrotactile stimulation were extensively investigated in literature [22], and this has been considered in the present study. The separation between the electrode pads (12 mm) was above the two-point spatial discrimination on the forearm (~9 mm [71]). Similarly, since the feedback relied on only four, equidistantly arranged, intensity levels, the separation between the levels was also well above the just noticeable difference in amplitude [72]. This ensured that the subjects would be able to detect the transition between adjacent electrode pads and amplitude levels. Previous studies investigating feedback used a similar number of location, amplitude and/or frequency levels, which were sometimes combined (mixed coding) to increase the feedback resolution [25,32,60,73]. A specific challenge in the present study, however, was that the electrotactile codes

corresponding to the two DoFs were simultaneously active, thereby possibly affecting the perception and interpretation [74]. Therefore, the previous results on optimal spatial and amplitude resolution for a single feedback variable could not be directly translated to a two DoF scenario. The four times four level coding schemes were selected based on pilot testing. Nevertheless, determining the optimal spatial and amplitude resolution when providing two feedback variables simultaneously is indeed an important future goal. Similarly, the coding could be extended to represent more feedback variables. For example, grasping force could be communicated by modulating the stimulation frequency of the hand aperture feedback [25]. This would allow communicating the full state of a multifunctional prosthesis, which is indeed an ultimate goal. The control was sequential in the present study since it was based on pattern classification. Therefore, although the subjects felt the sensations for two DoFs simultaneously, they could move only one DoF at a time. A relevant future step would be to evaluate the feedback schemes when using simultaneous control via regression [75].

## 5. Conclusion

This study investigated the effectiveness of two novel electrotactile feedback schemes using spatial and amplitude coding to communicate proprioceptive information about two DoFs simultaneously. The results of closed-loop myoelectric control showed that even with minimal training (< 30 minutes) a very good performance can be achieved with both configurations. In addition, the subjects reported that both feedback schemes were easily comprehensible and intuitive. The stimulation interface used to implement the feedback is compact, and therefore, it could be easily integrated in a two DoF myoelectric prosthesis, potentially enhancing the prosthesis utility and embodiment in users.

## Acknowledgements

The authors would like to thank the participants, who all participated voluntarily. This work has been supported by the projects 8022-00243A (ROBIN) and 8022-00226B funded by the Independent Research Fund Denmark and an EU funded project TACTILITY (H2020-ICT-25- 856718).

## References

- [1] Schofield J S, Evans K R, Carey J P and Hebert J S 2014 Applications of sensory feedback in motorized upper extremity prosthesis: A review *Expert Rev. Med. Devices* **11** 499–511
- [2] Østlie K, Magnus P, Skjeldal O H, Garfelt B and Tambs K 2011 Mental health and satisfaction with life among upper limb amputees: A Norwegian population-based survey comparing adult acquired

- major upper limb amputees with a control group  
*Disabil. Rehabil.* **33** 1594–607
- [3] Geethanjali P 2016 Myoelectric control of prosthetic hands : state-of-the-art review *Med. Devices Evid. Res.* **247–55**
- [4] Biddiss E A and Chau T T 2007 Upper limb prosthesis use and abandonment: A survey of the last 25 years *Prosthet. Orthot. Int.* **31** 236–57
- [5] Cordella F, Ciancio A L, Sacchetti R, Davalli A, Cutti A G, Guglielmelli E and Zollo L 2016 Literature Review on Needs of Upper Limb Prosthesis Users *Front. Neurosci.* **10** 1–14
- [6] Peerdeman B, Hermens H, Stramigioli S, Rietman H, Witteveen H, Huis in 't Veld R, Misra S, Veltink P and Boere D 2011 Myoelectric forearm prostheses: State of the art from a user-centered perspective *J. Rehabil. Res. Dev.* **48** 719–38
- [7] Pamungkas D and Ward K 2015 Electro-tactile feedback system for a prosthetic hand *22nd Annu. Int. Conf. Mechatronics Mach. Vis. Pract. M2VIP 2015* 27–38
- [8] Jorgovanovic N, Dosen S, Djozic D J, Krajoski G and Farina D 2014 Virtual grasping: Closed-loop force control using electrotactile feedback *Comput. Math. Methods Med.* **2014** 13pp
- [9] Witteveen H J B B, Luft F, Rietman J S and Veltink P H 2014 Stiffness feedback for myoelectric forearm prostheses using vibrotactile stimulation *IEEE Trans. Neural Syst. Rehabil. Eng.* **22** 53–61
- [10] Witteveen H J B, Rietman H S and Veltink P H 2015 Vibrotactile grasping force and hand aperture feedback for myoelectric forearm prosthesis users. *Prosthet. Orthot. Int.* **39** 204–12
- [11] Witteveen H J B B, Rietman J S and Veltink P H 2012 Grasping force and slip feedback through vibrotactile stimulation to be used in myoelectric forearm prostheses *Proc. Annu. Int. Conf. IEEE Eng. Med. Biol. Soc. EMBS* **2012** 2969–72
- [12] Clemente F, D'Alonzo M, Controzzi M, Edin B B and Cipriani C 2016 Non-Invasive, Temporally Discrete Feedback of Object Contact and Release Improves Grasp Control of Closed-Loop Myoelectric Transradial Prostheses *IEEE Trans. Neural Syst. Rehabil. Eng.* **24** 1314–22
- [13] Vincent Systems 2005 Vincent Evolution 2. Accessed 5 May 2020 from website: <https://vincentsystems.de/en/prosthetics/vincent-evolution-2/>
- [14] Antfolk C, D'Alonzo M, Rosén B, Lundborg G, Sebelius F, Cipriani C, Fredrik S and Cipriani C 2013 Sensory feedback in upper limb prosthetics *Expert Rev. Ltd* **10** 45–54
- [15] D'Anna E, Petrini F M, Artoni F, Popovic I, Simanić I, Raspopovic S and Micera S 2017 A somatotopic bidirectional hand prosthesis with transcutaneous electrical nerve stimulation based sensory feedback *Sci. Rep.* **7** 15pp
- [16] Vargas L, Shin H, Huang H, Zhu Y and Hu X 2019 Object stiffness recognition using haptic feedback delivered through transcutaneous proximal nerve stimulation *J. Neural Eng.* **17** 13pp
- [17] Petrini F M, Valle G, Strauss I, Granata G, Di Iorio R, D'Anna E, Čvančara P, Mueller M, Carpaneto J, Clemente F, Controzzi M, Bioni L, Carboni C, Barbaro M, Iodice F, Andreu D, Hiairassary A, Divoux J-L L, Cipriani C, Guiraud D, Raffo L, Fernandez E, Stieglitz T, Raspopovic S, Rossini P M and Micera S 2019 Six-Month Assessment of a Hand Prosthesis with Intraneural Tactile Feedback *Ann. Neurol.* **85** 137–54
- [18] Clemente F, Valle G, Controzzi M, Strauss I, Iberite F, Stieglitz T, Granata G, Rossini P M, Petrini F, Micera S and Cipriani C 2019 Intraneural sensory feedback restores grip force control and motor coordination while using a prosthetic hand *J. Neural Eng.* **16** 026034 (9pp)
- [19] Flesher S N, Collinger J L, Foldes S T, Weiss J M, Downey J E, Tyler-Kabara E C, Bensmaia S J, Schwartz A B, Boninger M L and Gaunt R A 2016 Intracortical microstimulation of human somatosensory cortex *Sci. Transl. Med.* **8** 361ra141
- [20] Tabot G A, Dammann J F, Berg J A, Tenore F V., Boback J L, Vogelstein R J and Bensmaia S J 2013 Restoring the sense of touch with a prosthetic hand through a brain interface *Proc. Natl. Acad. Sci.* **110** 18279–84
- [21] Szeto A Y J and Saunders F A 1982 Electrocutaneous Stimulation for Sensory Communication in Rehabilitation Engineering *IEEE Trans. Biomed. Eng.* **BME-29** 300–8
- [22] Kaczmarek K A, Webster J G, Bach-y-Rita P and Tompkins W J 1991 Electrotactile and vibrotactile displays for sensory substitution systems. *IEEE Trans. Biomed. Eng.* **38** 1–16
- [23] Franceschi M, Seminara L, Dosen S, Strbac M, Valle M and Farina D 2017 A System for Electrotactile Feedback Using Electronic Skin and Flexible Matrix Electrodes: Experimental Evaluation *IEEE Trans. Haptics* **10** 162–72
- [24] Geng B, Yoshida K, Petrini L and Jensen W 2012 Evaluation of sensation evoked by electrocutaneous stimulation on forearm in nondisabled subjects *J. Rehabil. Res. Dev.* **49** 297
- [25] Dosen S, Markovic M, Strbac M, Belic M, Kojic V, Bijelic G, Keller T, Farina D, Belić M, Kojić V, Bijelić G, Farina D and Keller T 2016 Multichannel Electrotactile Feedback With Spatial and Mixed Coding for Closed-Loop Control of Grasping Force in Hand Prostheses *IEEE Trans. Neural Syst. Rehabil. Eng.* **25** 183–95
- [26] Svensson P, Wijk U, Björkman A and Antfolk C 2017 A review of invasive and non-invasive sensory feedback in upper limb prostheses *Expert Rev. Med. Devices* **14** 439–47
- [27] Ingram H A, van Donkelaar P, Cole J, Vercher J-L L, Gauthier G M and Miall R C 2000 The role of

- 1  
2  
3 proprioception and attention in a visuomotor  
4 adaptation task *Exp. Brain Res.* **132** 114–26
- 5 [28] Schiefer M A, Graczyk E L, Sidik S M, Tan D W  
6 and Tyler D J 2018 Artificial tactile and  
7 proprioceptive feedback improves performance and  
8 confidence on object identification tasks ed M  
9 Sakakibara *PLoS One* **13** 1–18
- 10 [29] Horch K, Meek S, Taylor T G and Hutchinson D T  
11 2011 Object discrimination with an artificial hand  
12 using electrical stimulation of peripheral tactile and  
13 proprioceptive pathways with intrafascicular  
14 electrodes *IEEE Trans. Neural Syst. Rehabil. Eng.* **19**  
15 483–9
- 16 [30] Erwin A and Sup F C 2015 A haptic feedback  
17 scheme to accurately position a virtual wrist  
18 prosthesis using a three-node tactor array ed S J  
19 Bensmaia *PLoS One* **10** e0134095
- 20 [31] Battaglia E, Clark J, Bianchi M, Catalano M, Bicchi  
21 A and O'Malley M K 2019 Skin stretch haptic  
22 feedback to convey closure information in  
23 anthropomorphic, under-actuated upper limb soft  
24 prostheses *IEEE Trans. Haptics* **12** 508–20
- 25 [32] Štrbac M, Belić M, Isaković M, Kojić V, Bijelić G,  
26 Popović I, Radotić M, Došen S, Marković M, Farina  
27 D and Keller T 2016 Integrated and flexible  
28 multichannel interface for electrotactile stimulation  
29 *J. Neural Eng.* **13** 1–16
- 30 [33] Arakeri T J, Hasse B A and Fuglevand A J 2018  
31 Object discrimination using electrotactile feedback *J.*  
32 *Neural Eng.* **15** 12pp
- 33 [34] D'Anna E, Valle G, Mazzoni A, Strauss I, Iberite F,  
34 Patton J, Petrini F M, Raspopovic S, Granata G, Iorio  
35 R Di, Controzzi M, Cipriani C, Stieglitz T, Rossini P  
36 M and Micera S 2019 A closed-loop hand prosthesis  
37 with simultaneous intraneural tactile and position  
38 feedback *Sci. Robot.* **4** 13pp
- 39 [35] Scheme E J, Hudgins B S and Englehart K B 2013  
40 Confidence-based rejection for improved pattern  
41 recognition myoelectric control *IEEE Trans. Biomed.*  
42 *Eng.* **60** 1563–70
- 43 [36] Scheme E and Englehart K 2013 Validation of a  
44 selective ensemble-based classification scheme for  
45 myoelectric control using a three dimensional Fitts'  
46 law test *Neural Syst. Rehabil. Eng. IEEE Trans.* **21**  
47 616–23
- 48 [37] Wurth S M and Hargrove L J 2014 A real-time  
49 comparison between direct control, sequential pattern  
50 recognition control and simultaneous pattern  
51 recognition control using a Fitts' law style  
52 assessment procedure *J. Neuroeng. Rehabil.* **11** 1–13
- 53 [38] Kamavuako E N, Scheme E J and Englehart K B  
54 2014 On the usability of intramuscular EMG for  
55 prosthetic control: A Fitts' Law approach *J.*  
56 *Electromyogr. Kinesiol.* **24** 770–7
- 57 [39] Waris A, Mendez I, Englehart K, Jensen W and  
58 Kamavuako E N 2019 On the robustness of real-time  
59 myoelectric control investigations: A multiday Fitts'  
60 law approach *J. Neural Eng.* **16**
- [40] Mendez I, Hansen B W, Grabow C M, Smedegaard  
E J L, Skogberg N B, Uth X J, Bruhn A, Geng B and  
Kamavuako E N 2017 Evaluation of the Myo  
Armband for the Classification of hand motions *Int.*  
*Conf. Rehabil. Robot.* 1211–4
- [41] Visconti P, Gaetani F, Zappatore G A and Primiceri  
P 2018 Technical features and functionalities of Myo  
armband: An overview on related literature and  
advanced applications of myoelectric armbands  
mainly focused on arm prostheses *Int. J. Smart Sens.*  
*Intell. Syst.* **11** 1–25
- [42] Štrbac M, Isakovic M, Belic M, Popović I, Simanic  
I, Farina D, Keller T, Dosen S, Štrbac M, Isaković  
M, Belić M, Popović I, Simanić I, Farina D, Keller T  
and Došen S 2017 Short-and long-term learning of  
feedforward control of a myoelectric prosthesis with  
sensory feedback by amputees *IEEE Trans. Neural*  
*Syst. Rehabil. Eng.* **25** 2133–45
- [43] Witteveen H J B, Droog E A, Rietman J S and  
Veltink P H 2012 Vibro- and electrotactile user  
feedback on hand opening for myoelectric forearm  
prostheses *IEEE Trans. Biomed. Eng.* **59** 2219–26
- [44] Isaković M, Belić M, Došen S, Štrbac M, Popović I,  
Keller T and Farina D 2016 Electrotactile feedback  
improves performance and facilitates learning in the  
routine grasping task *Eur. J. Transl. Myol.* **26** 197–  
202
- [45] Patel G K, Dosen S, Castellini C and Farina D 2016  
Multichannel electrotactile feedback for  
simultaneous and proportional myoelectric control *J.*  
*Neural Eng.* **13** 13pp
- [46] Donovan I M, Puchin J, Okada K and Zhang X 2017  
Simple space-domain features for low-resolution  
sEMG pattern recognition *Proc. Annu. Int. Conf.*  
*IEEE Eng. Med. Biol. Soc. EMBS* 62–5
- [47] Hudgins B, Parker P and Scott R N 1993 A new  
strategy for multifunction myoelectric control *IEEE*  
*Trans. Biomed. Eng.* **40** 82–94
- [48] Menon R, Lakany H, Di Caterina G, Conway B A,  
Petropoulakis L and Soraghan J J 2017 Study on  
Interaction Between Temporal and Spatial  
Information in Classification of EMG Signals for  
Myoelectric Prostheses *IEEE Trans. Neural Syst.*  
*Rehabil. Eng.* **25** 1832–42
- [49] Celadon N, Do S, Binder I, Ariano P and Farina D  
2016 Proportional estimation of finger movements  
from high-density surface electromyography *J.*  
*Neuroeng. Rehabil.* **13** 1–19
- [50] Scheme E and Englehart K 2011 Electromyogram  
pattern recognition for control of powered upper-  
limb prostheses: State of the art and challenges for  
clinical use *J. Rehabil. Res. Dev.* **48** 643–60
- [51] Yang D, Gu Y, Thakor N V. and Liu H 2019  
Improving the functionality, robustness, and  
adaptability of myoelectric control for dexterous  
motion restoration *Exp. Brain Res.* **237** 291–311
- [52] Englehart K and Hudgins B 2003 A robust, real-time  
control scheme for multifunction myoelectric

- control. *IEEE Trans. Biomed. Eng.* **50** 848–54
- [53] Powell M A, Kaliki R R and Thakor N V. 2014 User training for pattern recognition-based myoelectric prostheses: Improving phantom limb movement consistency and distinguishability *IEEE Trans. Neural Syst. Rehabil. Eng.* **22** 522–32
- [54] Simon A M, Hargrove L J, Lock B A and Kuiken T A 2011 The Target Achievement Control Test: Evaluating real-time myoelectric pattern recognition control of a multifunctional upper-limb prosthesis *J. Rehabil. Res. Dev.* 619–627
- [55] Parker P, Englehart K and Hudgins B 2006 Myoelectric signal processing for control of powered limb prostheses *J. Electromyogr. Kinesiol.* **16** 541–8
- [56] Duda R O, Hart P E and Stork D G 2001 *Pattern Classification*
- [57] Fougner A, Stavadahl O, Kyberd P J, Losier Y G and Parker P A 2012 Control of upper limb prostheses: Terminology and proportional myoelectric control a review *IEEE Trans. Neural Syst. Rehabil. Eng.* **20** 663–77
- [58] Belter J T, Segil J L, Dollar A M and Weir R F 2013 Mechanical design and performance specifications of anthropomorphic prosthetic hands: a review. *J. Rehabil. Res. Dev.* **50** 599–618
- [59] Cipriani C, Segil J L, Clemente F, Richard R F and Edin B 2014 Humans can integrate feedback of discrete events in their sensorimotor control of a robotic hand *Exp. Brain Res.* **232** 3421–9
- [60] Schweisfurth M A, Markovic M, Dosen S, Teich F, Graimann B and Farina D 2016 Electrotactile EMG feedback improves the control of prosthesis grasping force *J. Neural Eng.* **13** 15pp
- [61] A.A. Kingdom F and Prins N 2009 *Psychophysics: A Practical Introduction* (Academic Press)
- [62] Štrbac M, Isaković M, Belić M, Popović I, Simanić I, Farina D, Keller T and Došen S 2017 Short- and long-term learning of feedforward control of a myoelectric prosthesis with sensory feedback by amputees *IEEE Trans. Neural Syst. Rehabil. Eng.* **25** 2133–45
- [63] Adams J A, Gopher D and Lintern G 1977 Effects of visual and proprioceptive feedback on motor learning *J. Mot. Behav.* **9** 11–22
- [64] Isakovic M, Malešević J, Keller T, Kostić M and Štrbac M 2019 Optimization of Semiautomated Calibration Algorithm of Multichannel Electrotactile Feedback for Myoelectric Hand Prosthesis *Appl. Bionics Biomech.* **2019**
- [65] Dosen S, Schaeffer M and Farina D 2014 Time-division multiplexing for myoelectric closed-loop control using electrotactile feedback *J. Neuroeng. Rehabil.* **11** 1–10
- [66] Hartmann C, Došen S, Amsuess S and Farina D 2015 Closed-loop control of myoelectric prostheses with electrotactile feedback: Influence of stimulation artifact and blanking *IEEE Trans. Neural Syst. Rehabil. Eng.* **23** 807–16
- [67] Chai G, Sui X, Li S, He L and Lan N 2015 Characterization of evoked tactile sensation in forearm amputees with transcutaneous electrical nerve stimulation *J. Neural Eng.* **12** 13pp
- [68] Saunders I and Vijayakumar S 2011 The role of feed-forward and feedback processes for closed-loop prosthesis control *J. Neuroeng. Rehabil.* **8** 60
- [69] Markovic M, Schweisfurth M A, Engels L F, Farina D and Dosen S 2018 Myocontrol is closed-loop control: Incidental feedback is sufficient for scaling the prosthesis force in routine grasping *J. Neuroeng. Rehabil.* **15** 11pp
- [70] Wilke M A, Niethammer C, Meyer B, Farina D and Dosen S 2019 Psychometric characterization of incidental feedback sources during grasping with a hand prosthesis *J. Neuroeng. Rehabil.* **16** 13pp
- [71] Solomonow M, Lyman J and Freedy A 1977 Electrotactile two-point discrimination as a function of frequency, body site, laterality, and stimulation codes *Ann. Biomed. Eng.* **5** 47–60
- [72] Dong J, Kamavuako E N, Dosen S, Jensen W and Geng B 2020 The Short-Term Repeatability of Subdermal Electrical Stimulation for Sensory Feedback *IEEE Access* **8** 63983–92
- [73] Anani A B, Ikeda K and Körner L M 1977 Human ability to discriminate various parameters in afferent electrical nerve stimulation with particular reference to prostheses sensory feedback *Med. Biol. Eng. Comput.* **15** 363–73
- [74] Geng B, Yoshida K and Jensen W 2011 Impacts of selected stimulation patterns on the perception threshold in electrocutaneous stimulation *J. Neuroeng. Rehabil.* **8** 9
- [75] Hahne J M, Markovic M and Farina D 2017 User adaptation in Myoelectric Man-Machine Interfaces *Sci. Rep.* **7** 1–10